JOURNAL OF AIRCRAFT
Vol. 32, No. 3, May–June 1995

Actuated Forebody Strake Controls for the F-18 High-Alpha Research Vehicle

Daniel G. Murri,* Gautam H. Shah,† and Daniel J. DiCarlo‡
NASA Langley Research Center, Hampton, Virginia 23681
and
Todd W. Trilling§
Lockheed Engineering and Sciences Company, Inc., Hampton, Virginia 23666

A series of ground-based studies have been conducted to develop actuated forebody strake controls for flight-test evaluations using the NASA F-18 High-Alpha Research Vehicle (HARV). The actuated forebody strakes were designed to provide increased levels of yaw control at high angles of attack where conventional rudders become ineffective. Results are presented from tests conducted with the flight-test strake design, including static and dynamic wind-tunnel tests, transonic wind-tunnel tests, full-scale wind-tunnel tests, pressure surveys, and flow visualization tests. Results from these studies show that a pair of conformal actuated forebody strakes applied to the F-18 HARV can provide a powerful and precise yaw control device at high angles of attack. The preparations for flight testing are described, including the fabrication of flight hardware and the development of aircraft flight control laws. The primary objectives of the flight tests are to provide flight validation of the ground-based studies and to evaluate the use of this type of control to enhance fighter aircraft maneuverability.

Nomenclature

The moment reference center for the wind-tunnel data is fuselage station 458.56 (25% mean aerodynamic chord) and water line 100.0.

b = reference wingspan, 37.42 ft (full scale)
C_L = lift coefficient, lift/$q_\infty S$
C_l = body-axis rolling-moment coefficient, rolling moment/$q_\infty Sb$
C_m = body-axis pitching-moment coefficient, pitching moment/$q_\infty S\bar{c}$
C_n = body-axis yawing-moment coefficient, yawing moment/$q_\infty Sb$
C_p = static pressure coefficient (local static pressure − freestream static pressure)/q_∞
C_Y = body-axis side-force coefficient, side force/$q_\infty S$
$\bar{c}$ = mean aerodynamic chord, 11.52 ft (full scale)
FS = fuselage station, full scale, in.
L = left
q_∞ = freestream dynamic pressure, lb/ft^2
R = right
S = reference wing area, 400 ft^2 (full scale)
V = freestream velocity, ft/s
α = angle of attack, deg
β = angle of sideslip, deg
δ_s = strake deflection measured from the retracted position, deg
$\delta_{s,d}$ = differential strake deflection, $\delta_{s,\text{right}} - \delta_{s,\text{left}}$, deg
Ω = rate of rotation about the velocity vector, rad/s

Introduction

A MAJOR goal of the NASA high-angle-of-attack technology program (HATP) has been to help develop technologies that can significantly improve the high-angle-of-attack controllability and maneuvering effectiveness of fighter aircraft. A wide range of advanced control concepts has been investigated under this program including propulsive control concepts as well as advanced aerodynamic control concepts. As part of the NASA HATP, flight tests have been conducted (Fig. 1) with a multiaxis thrust vectoring system applied to the NASA F-18 high-alpha research vehicle (HARV).[1] A follow-on series of flight tests with the NASA F-18 HARV will be focusing on the application of actuated forebody strake controls. These controls are designed to provide increased levels of yaw control at high angles of attack where conventional aerodynamic controls become ineffective. The series of flight tests are collectively referred to as the actuated nose strakes for enhanced rolling (ANSER) flight experiment. The

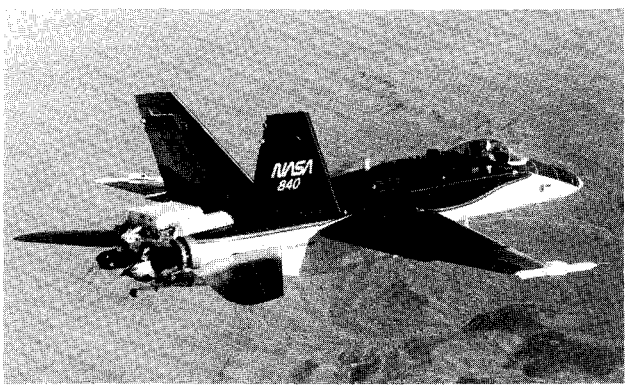

Fig. 1 Photograph of F-18 HARV.

Presented as Paper 93-3675 at the AIAA Atmospheric Flight Mechanics Conference, Monterey, CA, Aug. 9–11, 1993; received March 29, 1994; revision received Sept. 20, 1994; accepted for publication Oct. 3, 1994.

*Aerospace Technologist, Vehicle Dynamics Branch, Flight Dynamics and Control Division, M/S 355. Senior Member AIAA.
†Aerospace Technologist, Vehicle Dynamics Branch, Flight Dynamics and Control Division, M/S 355. Member AIAA.
‡Aerospace Technologist, Vehicle Performance Branch, Flight Dynamics and Control Division, M/S 247.
§Aerospace Engineer, Aeronautics and Management Support Group, Langley Program Office, Lockheed Engineering and Sciences Company, Inc., 144 Research Drive. Member AIAA.

ANSER acronym refers to "rolling" since the strakes provide the critical yaw control required to coordinate rolling maneuvers about the velocity vector at high-angle-of-attack conditions.

Following initial concept exploration, the actuated forebody strake concept has been refined through a wide range of studies to determine the suitability for flight testing on the F-18 HARV. Reference 2 presents an overview of these studies and describes the development of the strake design that has been accepted for flight testing. This article first summarizes the results of tests conducted with the flight-test strake design, including static and dynamic wind-tunnel tests, transonic wind-tunnel tests, full-scale wind-tunnel tests, pressure surveys, and flow visualization tests. The remainder of this article discusses the preparations for flight testing, including the fabrication of flight hardware, the development of aircraft flight control laws, and the flight-test objectives.

Background

Roll Control at High Angles of Attack

A major factor that limits the high-α maneuvering effectiveness of current fighter aircraft is the degradation of aerodynamic control effectiveness as angle of attack is increased. With these aircraft, rudder yaw-control power degrades rapidly as angle of attack approaches maximum lift due to the conventional rudder becoming immersed in the low-energy stalled wake shed from the wings and fuselage.[3] However, the level of yaw control required actually increases with angle of attack due to the increasing yaw rates required to coordinate the rolling maneuver about the velocity vector.[3] The typical result is that the level of yaw control required exceeds the amount available beginning at an angle of attack substantially lower than the angle of attack for maximum lift. The resulting deficiency in yaw control results in an inherent roll-rate limiting of the aircraft and, therefore, reduced maneuvering effectiveness.

An example of the roll-rate capability of the F-18 aircraft from Ref. 4 is presented in Fig. 2 and illustrates the reduction in roll performance that occurs as angle of attack is increased. The data of Fig. 2 show a large reduction in roll-rate capability from α = 0 to 20 deg, which is well below the angle of attack for maximum lift (between 35–40 deg). This reduction in roll-rate capability occurs largely because maximum roll control commands (aileron and differential stabilator) must be limited above α = 8 deg due to insufficient yaw control available to adequately coordinate the rolling maneuver.

Development of Strake Concept

There are several reasons for investigating advanced yaw control concepts that utilize the forebody. One reason is that fighter aircraft have evolved such that the moment arm from the forebody to the c.g. can be equal to or greater than the moment arm of the vertical tail(s). For the F-18 aircraft, the forebody moment arm is over two times the vertical tail moment arm. Another reason is that, as opposed to the vertical tails that are blanketed by stalled flow at high angles of attack, the forebody remains in undisturbed flow and is capable of producing a very powerful vortex flowfield. These considerations have led to a great deal of research on advanced control concepts designed to manipulate the forebody flowfield to provide the required yaw control at high-angle-of-attack conditions.

The typical forebody flowfield at high angles of attack is dominated by vortex flows, it can exhibit very nonlinear characteristics over small changes in flight condition, and it can be very highly coupled with downstream aircraft components. Therefore, the designer is faced with the technical challenge of providing the desired control characteristics by harnessing this powerful, but often unpredictable, flowfield. As measures of merit, there are a number of ways to judge the potential usefulness of a particular control device. In general, it is highly desirable that the control device be effective over a wide range of flight conditions (α, β, Mach, etc.), have minimal control coupling into other axes, exhibit minimum lags in the development of control forces, and provide well-behaved control linearity characteristics (no control reversal). The actuated forebody strake concept has been developed with the goal of providing these desired characteristics. If these basic characteristics are not met, then the control device could, at a minimum, be very difficult to implement in a flight control system or could be unpredictable to the pilot.

Concepts designed to generate yaw control by manipulating the forebody flowfield include both mechanical and pneumatic methods, some of which are illustrated in Fig. 3. References 2 and 5–9 describe several mechanical methods such as actuated forebody strakes and rotatable forebody tips. References 9–12 describe pneumatic methods of manipulating the forebody flowfield including jet and slot blowing, and suction through ports. The current studies have focused on the application of a pair of longitudinally-hinged conformal actuated forebody strakes to the F-18 HARV configuration.

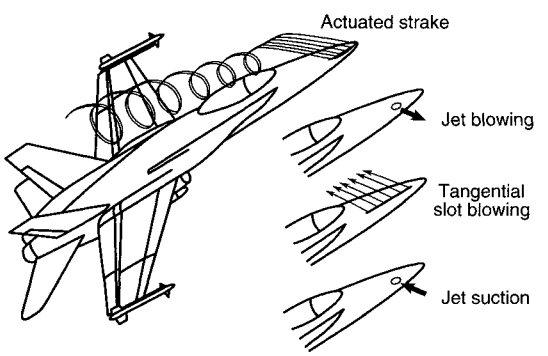

Fig. 3 Forebody flow control concepts.

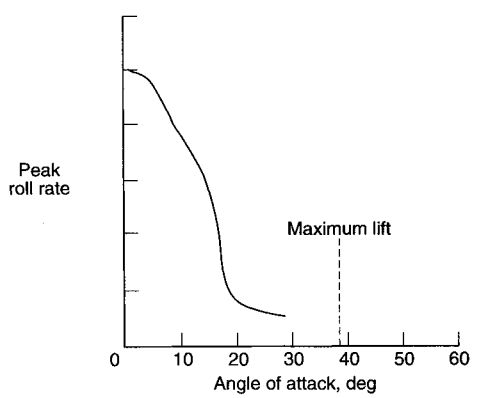

Fig. 2 F-18 roll-rate capability from Ref. 4, Mach number = 0.7, alt = 25,000 ft.

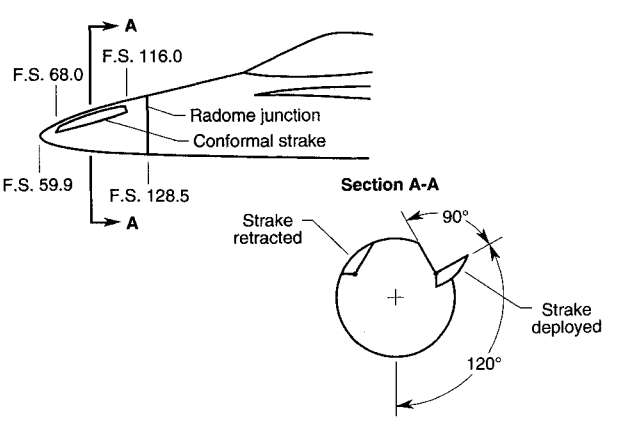

Fig. 4 ANSER strake design.

The overall development process of the actuated forebody strake concept has followed a successive series of studies from initial concept exploration to full-scale flight validation. The initial development tests of the actuated forebody strake concept were conducted using a generic fighter model and are described in Refs. 5 and 6. These tests showed that the actuated forebody strake concept could provide high levels of yaw control over wide ranges of angle of attack and sideslip and that the yawing moment could be controlled by varying the strake deflections. This concept has since been refined through a wide range of studies to develop the concept for application to the F-18 HARV and to support the planned flight tests.[2]

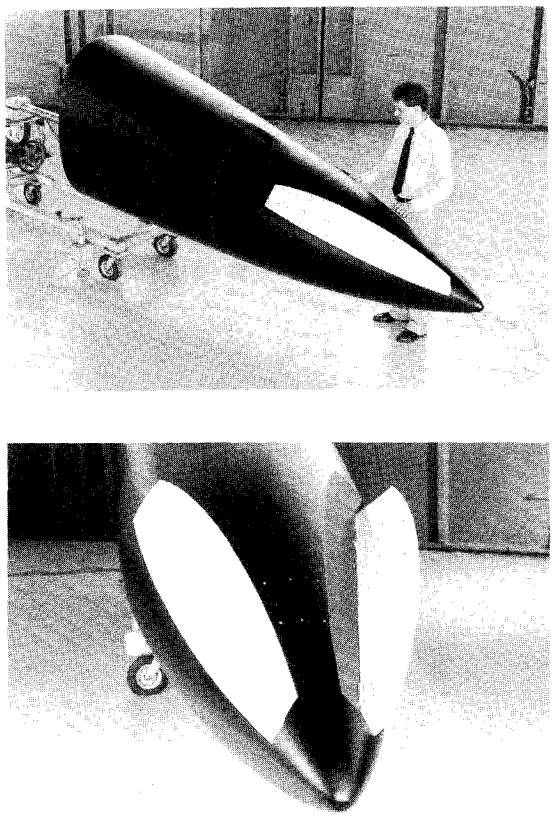

Fig. 5 Photographs of the ANSER strake design applied to the full-scale F-18 forebody wind-tunnel model: a) three-quarter front view and b) closeup of strakes.

A sketch of the conformal actuated forebody strakes designed for flight testing on the F-18 HARV is presented in Fig. 4. In addition, photographs of the strakes applied to a full-scale F-18 forebody wind-tunnel model are shown in Fig. 5. This strake design includes a pair of conformal actuated strakes, each capable of a 90-deg deflection and positioned at a radial location of 120 deg from the bottom of the forebody. The term "conformal" indicates that when both strakes are retracted, the forebody retains the nominal F-18 HARV forebody contour. In order to minimize the cost and difficulty of the aircraft modifications, the strakes are positioned to remain within the length of the radome of the full-scale F-18 HARV. The aircraft will be modified by attaching a newly fabricated radome incorporating the strakes and actuators and making the appropriate connections to the aircraft systems.

Description of Tests

The primary ground tests used in the analysis of the ANSER strake design are shown in Fig. 6. The tests include low-speed static and dynamic force tests using a 16%-scale model in the Langley 30- by 60-ft tunnel, transonic tests using a 6%-scale model in the David Taylor 7- by 10-ft transonic tunnel, rotary balance tests using a 10%-scale model in the Langley 20-ft vertical spin tunnel, full-scale F-18 forebody model tests in the Langley 30- by 60-ft tunnel, full-scale F-18 airframe tests in the Ames 80- by 120-ft tunnel, and free spinning tests using a 3.6%-scale model in the Langley 20-ft vertical spin tunnel. Both the 16%-scale model and the full-scale F-18 forebody model incorporated the fully conformal actuated strakes as shown in Figs. 4 and 5. The other models incorporated fixed strakes to simulate deployments of the conformal actuated strakes. All of the wind-tunnel data presented (except for the full-scale forebody results) were obtained with a wing leading-edge flap deflection of 34 deg (leading edge down) and a horizontal stabilator deflection of −12 deg (trailing edge up). Selected results are presented from these tests to provide an overview of the aerodynamic characteristic of the strakes.

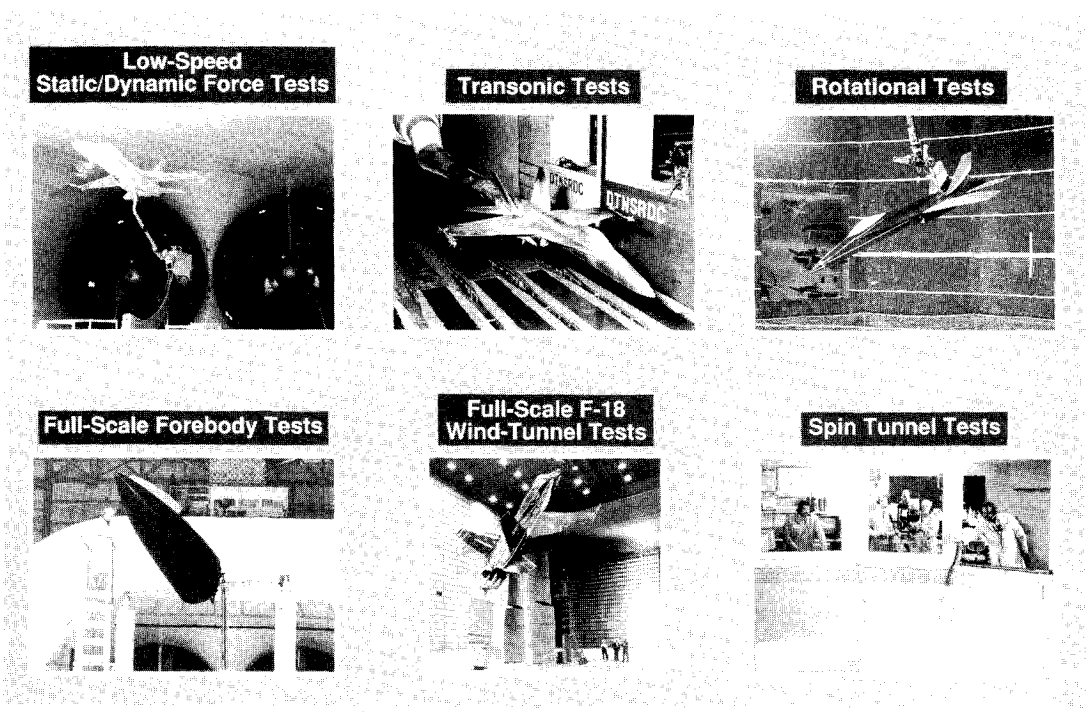

Fig. 6 Ground tests conducted in support of the ANSER flight experiment.

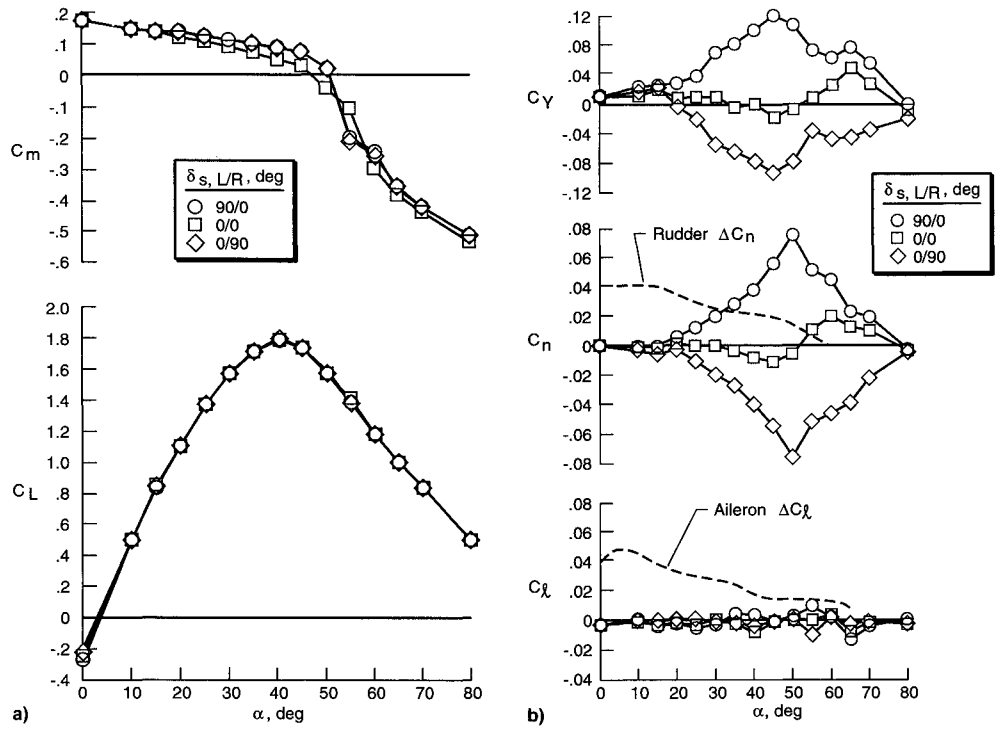

Fig. 7 Strake effectiveness characteristics, 16%-scale model, q_∞ = 10 lb/ft², Langley 30- by 60-ft tunnel: a) longitudinal and b) lateral-directional characteristics.

During the strake development process, additional studies were conducted with a preliminary version of the ANSER strake design. These studies are described in Ref. 2 and included wind-tunnel free-flight tests and preliminary piloted simulation studies, both of which illustrated the enhancements in controllability and maneuverability provided by the strakes. Computational fluid dynamics studies have also been conducted for the same preliminary strake configuration[13] and are continuing with the current ANSER strake design.

Results

Low-Speed Tests

The strake development tests showed that the maximum control effectiveness is obtained with an individual strake deflection of 90 deg. The effects of maximum strake deflections (90/0 and 0/90) on the longitudinal and lateral-directional characteristics of the 16%-scale model are presented in Fig. 7. Also shown in Fig. 7 are the incremental yawing moments produced by maximum rudder deflection (−30 deg) and the incremental rolling moments produced by maximum aileron deflection (−25 deg). As mentioned previously, conventional rudders lose effectiveness as stall develops due to the vertical tails becoming immersed in the low-energy stalled wake shed from the wings and fuselage. As compared to the rudder effectiveness that degrades rapidly above α = 20 deg, the yaw control provided by strakes increases and produces very high levels of yawing moment at higher angles of attack. Another important characteristic is that, even though they generate very high levels of yaw control, the strakes produce relatively small coupled rolling and pitching moments and have very little effect on lift. This low level of coupling in the other axes is very desirable and indicates that the strakes act essentially as a decoupled yaw control device.

The data of Fig. 7 also show that, without any yaw control deflection, the 16% scale model exhibits some moderate yawing moment and side force asymmetries beginning at about α = 30 deg. These asymmetries are typical of slender-body configurations and are due to asymmetric flow development on the forebody at high angles of attack. An important characteristic is that the yawing moments generated by the strakes

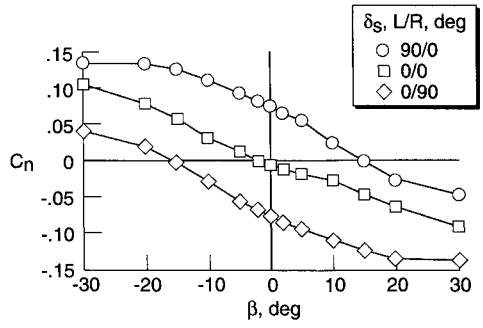

Fig. 8 Strake effectiveness at sideslip, α = 50 deg, 16%-scale model, q_∞ = 10 lb/ft², Langley 30- by 60-ft tunnel.

are not just superimposed on these natural asymmetries, but rather overpower the asymmetries to provide essentially identical control effectiveness in either direction.

The strake control characteristics vs β are presented in Fig. 8 for an angle of attack of 50 deg, and illustrate that the strakes provide yaw control increments over wide ranges in sideslip. This characteristic is especially important at the higher angle of attack conditions where perturbations in sideslip during maneuvering may be more pronounced than at lower angles of attack.

The strake control linearity characteristics are shown in Fig. 9 for angles of attack of α = 30 and 50 deg. Figure 9 shows the variation in yawing moment vs the differential strake deflection, as well as the individual strake deployments that make up the differential deflections. The differential strake deflection is given by $\delta_{s,d} = (\delta_{s,\text{right}} - \delta_{s,\text{left}})$ and represents the overall strake yaw-control deflection. At α = 30 deg, differential strake deflections are utilized such that one strake is deployed at a time. In this case, the data of Fig. 9a show that an almost linear variation of yawing moment is obtained at α = 30 deg with this strake deflection schedule.

During development tests, it was found that at higher angles of attack, deflecting one strake at a time could result in a small but undesirable control reversal at small strake deployments. To overcome this characteristic, a solution was de-

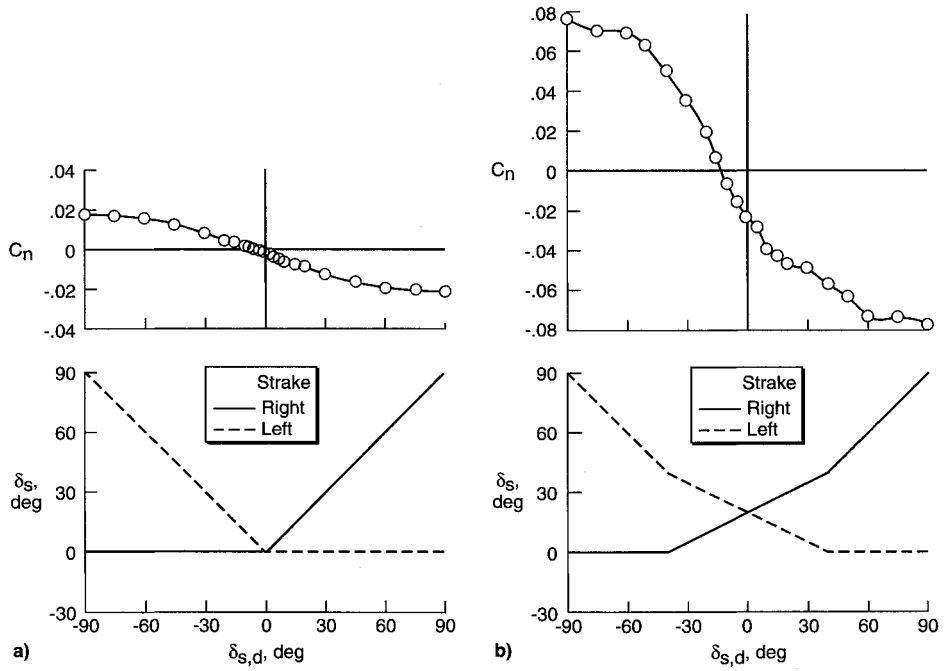

Fig. 9 Strake control-linearity characteristics, 16%-scale model, q_∞ = 10 lb/ft², Langley 30- by 60-ft tunnel: α = a) 30 and b) 50 deg.

veloped that deploys the strakes symmetrically as angle of attack increases above α = 30 deg. When a yawing moment is desired under these conditions, the strakes would then be deflected differentially about the symmetric strake deployment. For all angles of attack, however, the maximum yaw-control deflection would always consist of one strake fully deployed (δ_s = 90 deg) and the other strake fully retracted (δ_s = 0 deg).

Figure 9b shows the strake deflection schedule and resulting yawing moment characteristics at α = 50 deg. At this angle of attack, the strakes are deflected differentially from a symmetric deployment of δ_s = 20 deg on each side. Without any yaw control deflection ($\delta_{s,d}$ = 0 deg), the yawing-moment asymmetry that was described earlier is still evident, indicating that the symmetric deployment does not overcome the natural flow asymmetry. However, the use of this strake deployment schedule does provide a well-behaved variation of yawing moment with differential strake deflection. In general, these data show that the strakes can provide very desirable control linearity characteristics when implementing the proper strake deployment schedule.

Transonic Tests

Data demonstrating the effects of compressibility on the strake yaw-control characteristics are presented in Fig. 10. At angles of attack above α = 30 deg, the data show a reduction in strake yaw control effectiveness with increasing Mach number. The reductions in control effectiveness are relatively minor from M_∞ = 0.2 to 0.6, but more significant from M_∞ = 0.6 to 0.9 at angles of attack above α = 35 deg. These characteristics at the higher Mach numbers, however, would not be expected to have a major impact on the aircraft control effectiveness, since Mach numbers of approximately 0.8 or higher would be unobtainable at angles of attack above α = 35 deg (except at altitudes above 30,000 ft), because of structural "g" limits. A more detailed discussion of the Mach number effects on the strake control characteristics can be found in Ref. 14.

Rotary Balance Tests

Another important characteristic that should be considered is whether the level of strake yaw control effectiveness is retained after a roll maneuver has been initiated and the airplane is rolling about the velocity vector. These characteristics were determined using rotary balance tests. The results shown in Fig. 11 indicate that the increments in yaw control provided by the strakes are retained over a wide range of rotation rate.

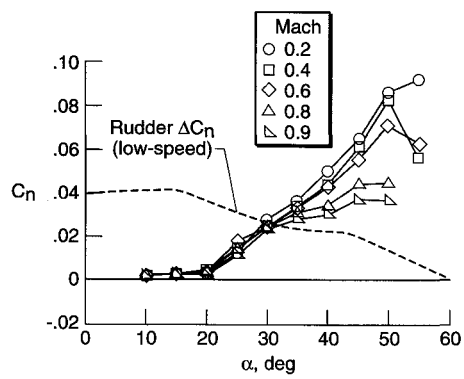

Fig. 10 Effect of Mach number on strake effectiveness, δ_s, L/R = 90/0, 6%-scale model, David Taylor 7- by 10-ft transonic tunnel.

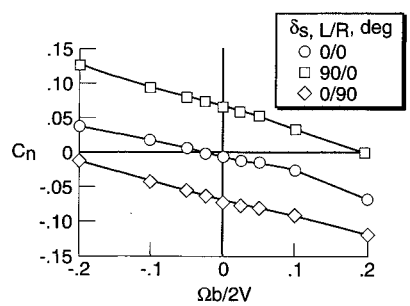

Fig. 11 Effect of rotation rate on strake effectiveness, α = 50 deg, 10%-scale model, q_∞ = 0.75 lb/ft², Langley 20-ft vertical spin tunnel.

Full-Scale Forebody Tests

Flow visualization and pressure distribution results were obtained with the full-scale F-18 forebody model and are used to describe the basic aerodynamic mechanisms that are responsible for the yawing moments generated by the strakes. The photographs in Fig. 12 were obtained using a laser light sheet technique and show head-on views of the forebody

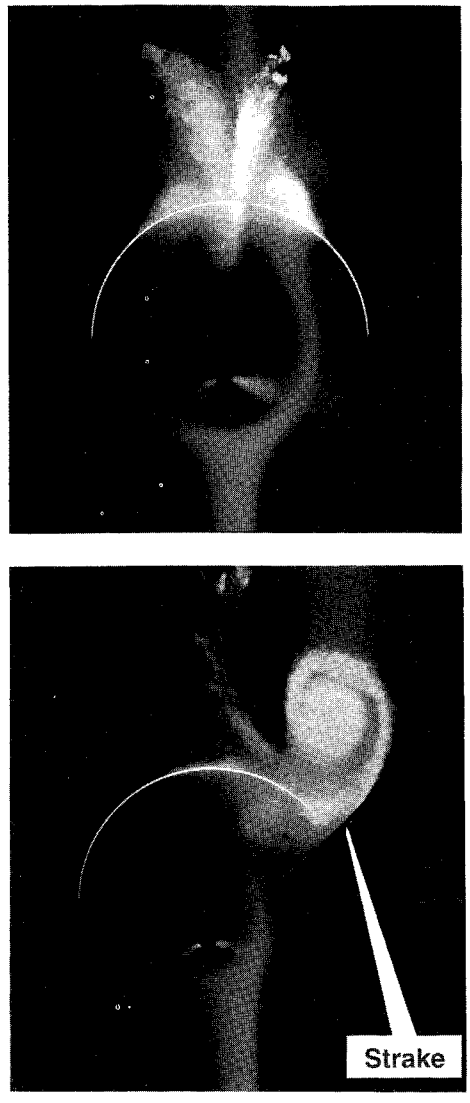

Fig. 12 Effect of strake deployment on forebody crossflow characteristics. Head-on view of full-scale F-18 forebody model, α = 50 deg, *FS* 107, q_∞ = 2 lb/ft^2, Langley 30- by 60-ft tunnel: a) strakes retracted and b) strake deployed 90 deg.

crossflow characteristics at α = 50 deg and *FS* 107.0 (about 80% down the length of the strake). With the strakes retracted, the photograph shows that the flow has separated symmetrically to produce a pair of small counter-rotating forebody vortices. However, with a maximum strake deployment, the photograph shows that the strake generates a much larger vortex, located above the strake and displaced away from the forebody.

The sketches in Fig. 13 show pressure distributions measured around the forebody for the same conditions shown in the photographs. With the strakes retracted, large suction pressures develop as the flow accelerates around the sides of the forebody. The flow then separates and the "footprints" of the two small vortices are evident on the top of the forebody. When a strake is deployed, the suction pressures are reduced on the strake-deployed side of the forebody and the suction pressures are increased on the strake-retracted side. Although it is not shown here, the increased suction pressures on the strake-retracted side of the forebody are accompanied by a delay in the primary separation line (visualized using oil flow). Therefore, it appears that a strake deployment generates a dominant vortex, forces separation and decelerates the flow on the strake-deployed side, and delays separation and accelerates the flow on the strake-retracted side. These changes in flow velocity generate differential suction pressures

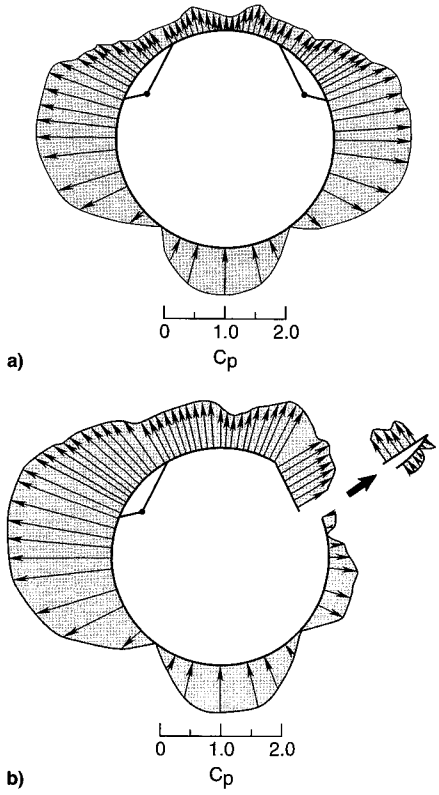

Fig. 13 Effect of strake deployment on forebody pressure distribution, full-scale F-18 forebody model, α = 50 deg, *FS* 107, q_∞ = 13 lb/ft^2, Langley 30- by 60-ft tunnel: a) strakes retracted and b) strake deployed 90 deg.

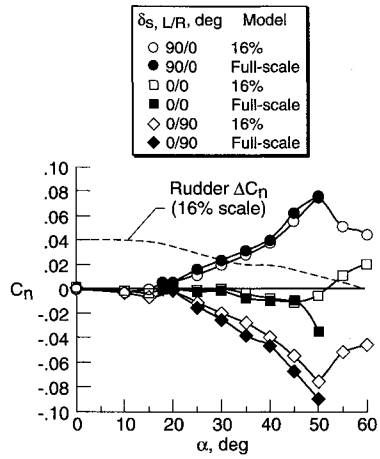

Fig. 14 Comparison of full-scale and 16%-scale strake effectiveness. Full scale from Ames 80- by 120-ft tunnel, q_∞ = 33 lb/ft^2. 16% scale from Langley 30- by 60-ft tunnel, q_∞ = 10 lb/ft^2.

that produce side forces and yawing moments in the direction away from the strake deployment.

Full-Scale F-18 Airframe Wind-Tunnel Tests

Strake effectiveness characteristics were also obtained during tests of a full-scale F-18 airframe in the Ames 80- by 120-ft tunnel. These tests are discussed in Ref. 9 and were conducted with "bolt-on" strakes that represented the maximum deployment of the conformal actuated strakes. The results shown in Fig. 14, in general, show very good agreement in maximum yaw control capability between the full-scale and 16%-scale test results. The full-scale results show slightly higher yaw-control effectiveness, which may be due to a delay in separation on the strake-retracted side of the forebody at the higher Reynolds number conditions.

Although not presented here, these tests also showed other desirable characteristics similar to those exhibited by the 16%-scale model. In particular, that the strakes maintain effectiveness over a wide range of sideslip and produce minimal coupling in the other axes. The control linearity characteristics could not be adequately assessed with the full-scale F-18 airframe during these tests because of the use of bolt-on strakes. Follow-on tests to address these characteristics have recently been completed in the 80- by 120-ft tunnel, but the results were not available in time to be included in this article. These follow-on tests utilized the same F-18 airframe as the earlier tests, except that the forebody was modified to incorporate the fully conformal ANSER strake design.

Flight-Test Preparations

Flight Hardware Fabrication

As described previously, the approach that is being taken to modify the F-18 HARV for the ANSER flight experiment is to replace the basic radome with a newly fabricated radome that incorporates the strakes, actuators, and instrumentation. The radome and strake flight hardware have been designed and fabricated at NASA Langley and are shown in Fig. 15. The radome and strake structures consist of aluminum skin panels that are riveted to aluminum stringers and bulkheads. Fiberglass fairings are used in several areas, but are not used as load-bearing components.

The hydraulic actuators used to drive the strakes consist of F-18 aileron actuators that have been modified for longer stroke, higher rate, and less force capability. The strake actuators have a stroke of ± 2.84 in. that provides each strake with a deflection of 0–90 deg. Based on the hinge moment measurements obtained during wind-tunnel testing, the strake actuators have been designed to provide a rate capability of 180 deg/s under the highest expected strake loads. This control surface rate allows a maximum strake deployment in $\frac{1}{2}$ s, which is the same time required for a maximum rudder deflection (30-deg deflection at 60 deg/s).

With a projected area of 2.71 ft^2 (each), the strakes are much smaller than any other aerodynamic control surface on the F-18 HARV. For example, each F-18 aileron has an area of approximately 12.2 ft^2 and each rudder has an area of approximately 8.1 ft^2. Therefore, much less force capability is required for the strake actuator (approximately 3300 lb) than for the F-18 aileron or rudder actuators, which provide approximately 12,100 and 13,900 lb, respectively.

Flight Hardware Instrumentation

In addition to the existing instrumentation system on the F-18 HARV, the newly fabricated radome will incorporate specific instrumentation required for the ANSER flight experiment. A total of 215 pressure orifices have been installed to provide surface pressure distributions around the radome, on the strakes, and on the nosecap. Assessment of radome structural loads and strake hinge moments will be provided by strain gauge measurements, and vibration information associated with the strakes will be obtained using accelerometers. In addition, a smoke port will be incorporated on each side of the radome and will be connected to the existing F-18 HARV smoke generating system[15] to allow visualization of the forebody and strake vortex flowfields.

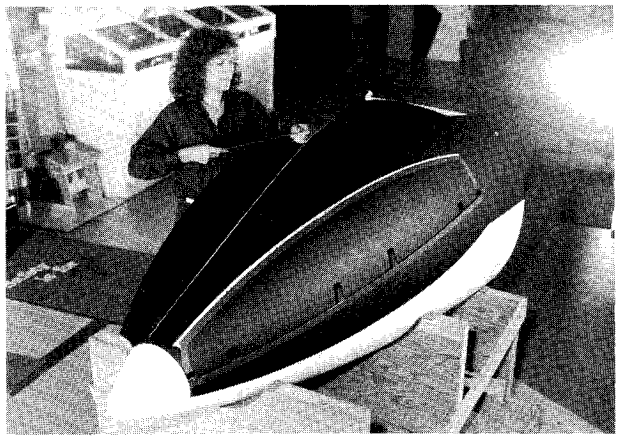

Fig. 15 Photograph of radome and strake flight hardware.

Development of Aircraft Flight Control Laws

In addition to the actuated forebody strakes, the thrust vectoring control system[1] that is currently installed on the F-18 HARV will be retained during the ANSER flight experiment. Because of this, a versatile set of flight control laws have been developed that will allow several combinations of advanced control concepts to be compared directly with the basic F-18 capabilities. The control laws have been developed utilizing an advanced design methodology[16] incorporating analytical synthesis techniques combined with nonlinear piloted simulation using the Langley differential maneuvering simulator.

These flight control laws will be implemented using the existing research flight control system[1] on the F-18 HARV and will include four research modes: 1) control augmentation using strakes (including pitch thrust vectoring), 2) control augmentation using multiaxis thrust vectoring, 3) control augmentation using strakes and multiaxis thrust vectoring, and 4) a programmed strake mode. The first control law mode is designed to evaluate yaw-control augmentation using strakes only. Pitch thrust vectoring is used in this mode, however, to allow the aircraft to trim at higher angles of attack than possible with aerodynamic controls alone. The second control law mode (with strakes deactivated) is the same set of advanced thrust-vectoring control laws recently evaluated on the F-18 HARV. This control law mode will be retained during the ANSER flight experiment to allow a direct comparison between strake augmentation and thrust vectoring augmentation. The third control law mode combines strakes and multiaxis thrust vectoring to provide the maximum potential agility. The fourth control mode is designed primarily to obtain aerodynamic data (control effectiveness, pressures, hinge moments, flow visualization) with varying strake deflections. This mode will allow preprogrammed deflections of the strakes and will use the thrust vectoring system to maintain a stabilized aircraft flight condition.

Flight-Test Objectives

The primary objectives of the ANSER flight experiment are to provide flight validation of a ground-test database for a forebody control device and to evaluate the use of this type of control to enhance fighter aircraft maneuverability. One focus of the flight tests will be on obtaining aerodynamic measurements (strake control effectiveness, surface pressures, hinge moments, and flow visualization) for comparison with ground-test results. Wind-tunnel free-flight tests and simulation studies have already given an indication that the strakes can provide significant enhancements in maneuverability.[2] However, another focus of the flight tests will be to evaluate the overall payoffs in agility and controllability obtainable with this type of control.

In addition to the primary flight test objectives, many other important integration issues are being addressed that could aid in future application of forebody control concepts. Some of the issues that are being addressed include control law design implications, hydraulic/actuator requirements, structural loads, aircraft systems integration considerations, and pilot acceptance of the unique response characteristics of the strakes.

Concluding Remarks

A wide range of coordinated ground-based studies are being used in the development of the actuated forebody strake control concept. Favorable results from these studies indicate that the ANSER strake design provides a powerful and precise yaw control device at high angles of attack. Although these studies are being applied to a specific forebody controls concept, they are providing an overall understanding of forebody controls characteristics and design implications. The primary objectives of the ANSER flight experiment are to provide flight validation of the ground-based studies and to evaluate the use of this type of control to enhance fighter aircraft maneuverability.

References

[1]Regenie, V., Gatlin, D., Kempel, R., and Matheny, N., "The F-18 High Alpha Research Vehicle: A High-Angle-of-Attack Testbed Aircraft," NASA TM-104253, Sept. 1992.

[2]Murri, D. G., Biedron, R. T., Erickson, G. E., Jordan, F. L., Jr., and Hoffler, K. D., "Development of Actuated Forebody Strake Controls for the F-18 High Alpha Research Vehicle," NASA CP-3149, Nov. 1990, pp. 335–380.

[3]Nguyen, L. T., "Flight Dynamics Research for Highly Agile Aircraft," Society of Automotive Engineers, SAE-89-2235, Sept. 1989.

[4]Schneider, E. T., and Meyer, R. R., Jr., "F-18 High Alpha Research Vehicle Description, Results, and Plans," *Thirty-Third Symposium Proceedings of the Society of Experimental Test Pilots*, 1989, pp. 135–162.

[5]Murri, D. G., "Wind-Tunnel Investigation of Actuated Forebody Strakes for Yaw Control at High Angles of Attack," M.S. Thesis, George Washington Univ., Washington, DC, May 1987.

[6]Murri, D. G., and Rao, D. M., "Exploratory Studies of Actuated Forebody Strakes for Yaw Control at High Angles of Attack," *Proceedings of the AIAA Atmospheric Flight Mechanics Conference* (Monterey, CA), 1987, pp. 279–295 (AIAA Paper 87-2557).

[7]Moskovitz, C., Hall, R., and DeJarnette, F., "Experimental Investigation of a New Device to Control the Asymmetric Flowfield on Forebodies at Large Angles of Attack," AIAA Paper 90-0069, Jan. 1990.

[8]Suárez, C. J., Kramer, B. R., and Malcolm, G. N., "Forebody Vortex Control on an F/A-18 Using Small Rotatable Tip-Strakes," *Proceedings of the AIAA 11th Applied Aerodynamics Conference* (Monterey, CA), 1993, Pt. 1, pp. 398–408 (AIAA Paper 93-3450).

[9]Lanser, W. R., and Murri, D. G., "Wind Tunnel Measurements on a Full-Scale F/A-18 with Forebody Slot Blowing or Forebody Strakes," AIAA Paper 93-1018, Feb. 1993.

[10]Guyton, R. W., and Maerki, G., "X-29 Forebody Jet Blowing," AIAA Paper 92-0017, Jan. 1992.

[11]Schreiner, J. A., Erickson, G. E., and Guyton, R., "Application of Tangential Sheet Blowing on the Forebody of an F-18-Like Configuration for High Angle-of-Attack Maneuverability," NASA CP-3150, Nov. 1990, pp. 1–26.

[12]White, E. R., "Effects of Suction on High-Angle-of-Attack Directional Control Characteristics of Isolated Forebodies," NASA CP-3149, Nov. 1990, pp. 533–556.

[13]Biedron, R. T., and Thomas, J. L., "Navier Stokes Computations for an F-18 Forebody with Actuated Control Strake," NASA CP-3149, Nov. 1990, pp. 481–506.

[14]Erickson, G. E., and Murri, D. G., "Wind Tunnel Investigations of Forebody Strakes for Yaw Control on F/A-18 Model at Subsonic and Transonic Speeds," NASA TP-3360, Sept. 1993.

[15]Fisher, D. F., Del Frate, J. H., and Richwine, D. M., "In-Flight Flow Visualization Characteristics of the NASA F-18 High Alpha Research Vehicle at High Angles of Attack," NASA TM-4193, May 1990.

[16]Davidson, J. B., Foster, J. V., Ostroff, A. J., Lallman, F. J., Murphy, P. C., Hoffler, K. D., and Messina, M. D., "Development of a Control Law Design Process Utilizing Advanced Synthesis Methods with Application to the NASA F-18 HARV," NASA CP-3137, Vol. 4, April 1992, pp. 111–157.